Experimentally excellent beaming in a two-layer dielectric structure

Anna C. Tasolamprou,[1,*] Lei Zhang,[2] Maria Kafesaki,[2,3] Thomas Koschny,[2] Costas M. Soukoulis[1,2]

[1] *Institute of Electronic Structure and Laser, FORTH, 71110, Heraklion, Crete, Greece*
[2] *Ames Laboratory and Department of Physics and Astronomy, Iowa State University, Ames, Iowa 50011, USA*
[3] *Department of Materials Science and Technology, University of Crete, 71003, Heraklion, Crete, Greece*

[*]*atasolam@iesl.forth.gr*

Abstract: We demonstrate both experimentally and theoretically that a two-layer dielectric structure can provide collimation and enhanced transmission of a Gaussian beam passing through it. This is due to formation of surface localized states along the layered structure and the coupling of these states to outgoing propagating waves. A system of multiple cascading two-layers can sustain the beaming for large propagation distances.

© 2014 Optical Society of America

OCIS codes: (050.5298) Photonic crystals; (240.6680) Surface plasmons; (050.2770) Gratings.

References and links

1. L. Martin-Moreno, F. J. Garcia-Vidal, H. J. Lezec, A. Degiron, and T. W. Ebbesen, "Theory of highly directional emission from a single subwavelength aperture surrounded by surface corrugations," Phys. Rev. Lett. **90**, 167401 (2003).
2. H. J. Lezec, A. Degiron, E. Devaux, R. A. Linke, L. Martin-Moreno, F. J. Garcia-Vidal, and T. W. Ebbesen, "Beaming light from a subwavelength aperture," Science **297**, 820–822 (2002).
3. J. Bravo-Abad, F. Garca-Vidal, and L. Martn-Moreno, "Wavelength de-multiplexing properties of a single aperture flanked by periodic arrays of indentations," Phot. and Nano. - Fund. and Appl. **1**, 55–62 (2003).
4. A. Çetin, K. Güven, and O. Müstecaplioglu, "Active control of focal length and beam deflection in a metallic nanoslit array lens with multiple sources," Opt. Lett. **35**, 1980–1982 (2010).
5. H. Caglayan, I. Bulu, and E. Ozbay, "Off-axis beaming from subwavelength apertures," J. Appl. Phys. **104**, 073108 (2008).
6. S. Kim, H. Kim, Y. Lim, and B. Lee, "Off-axis directional beaming of optical field diffracted by a single subwavelength metal slit with asymmetric dielectric surface gratings," Appl. Phys. Lett. **90**, 051113 (2007).
7. R. D. Meade, K. D. Brommer, A. M. Rappe, and J. D. Joannopoulos, "Electromagnetic bloch waves at the surface of a photonic crystal," Phys. Rev. B **44**, 10961–10964 (1991).
8. G. Arjavalingam, W. Robertson, R. Meade, K. Brommer, A. Rappe, and J. Joannopoulos, "Observation of surface photons on periodic dielectric arrays," Opt. Lett. **18**, 528–530 (1993).
9. F. Ramos-Mendieta and P. Halevi, "Surface modes in a 2d array of square dielectric cylinders," Solid State Commun. **100**, 311–314 (1996).
10. I. Bulu, H. Caglayan, and E. Ozbay, "Beaming of light and enhanced transmission via surface modes of photonic crystals," Opt. Lett. **30**, 3078–3080 (2005).
11. R. Moussa, B. Wang, G. Tuttle, T. Koschny, and C. M. Soukoulis, "Effect of beaming and enhanced transmission in photonic crystals," Phys. Rev. B **76**, 235417 (2007).
12. S. K. Morrison and Y. S. Kivshar, "Engineering of directional emission from photonic-crystal waveguides," Appl. Phys. Lett. **86**, 081110 (2005).
13. P. Kramper, M. Agio, C. M. Soukoulis, A. Birner, F. Müller, R. B. Wehrspohn, U. Gösele, and V. Sandoghdar, "Highly directional emission from photonic crystal waveguides of subwavelength width," Phys. Rev. Lett. **92**, 113903 (2004).

14. B. Wang, W. Dai, A. Fang, L. Zhang, G. Tuttle, T. Koschny, and C. M. Soukoulis, "Surface waves in photonic crystal slabs," Phys. Rev. B **74**, 195104 (2006).
15. W. Dai and C. Soukoulis, "Converging and wave guiding of gaussian beam by two-layer dielectric rods," Appl. Phys. Lett. **93**, 201101 (2008).
16. "https://www.comsol.com".
17. K. M. Ho, C. T. Chan, and C. M. Soukoulis, "Existence of a photonic gap in periodic dielectric structures," Phys. Rev. Lett. **65**, 3152–3155 (1990).
18. P. Markos and C. Soukoulis, *Wave Propagation: From Electrons to Photonic Crystals and Left-handed Materials* (Princeton University, 2008).

1. Introduction

Highly directional light emission has been found to occur in metallic subwavelength apertures when the metal surrounding them features surface corrugations [1, 2]. The enhanced directionality and transmission is is due to these surface corrugations that enable the coupling of the highly confined at the metal surface and non-radiative surface plasmon polaritons to outgoing propagating modes. Beaming in metallic structures is extensively investigated and various configurations for the manipulation of the propagating waves have been proposed [3–6]. In analogy to the surface plasmon polaritons which under certain conditions propagate strongly bound to a metal-dielectric interface, it has been shown that similar surface states can be supported by dielectric photonic crystals [7–10]. The excitation of the surface waves in photonic crystals requires the appropriate termination of the bulk periodic structure which may consist of a modified layer with different geometrical parameters than those of the bulk photonic crystal. Similarly to the metallic surface corrugations, a layer of scatterers on top of the modified layer, often call grating layer, facilities the coupling of the surface waves to radiation modes and results in enhanced beaming [11–13]. Apart from the photonic crystals, it has been discovered that even a single dielectric layer can support such surface states, i.e. states extended along the layer and localized in the perpendicular direction [14]. The surface states in this case are nothing else than the resonant guided mode of the dielectric layer. Placing a proper additional grating layer provides coupling to the radiation modes and directional propagation and by using several two-layer structures, also referred as bilayers, the beaming can be sustained for long distances. In 2008, Dai *et al*. [15], demonstrated theoretically that a multiple bilayer dielectric structure may give excellent beaming and enhanced transmission simultaneously of a Gaussian source. The first layer of each bilayer supports surface states and the rear, grading layer couples the surface states to radiation modes. It has been proven that multiple bilayers can enforce and sustain the collimation and high transmission at long distances. This paper presents the experimental proof of the bilayers converging and guiding ability and a numerical analysis which further supports the argument. The experiments are conducted in the microwave regime involving mm-scale structures. Given that the materials involved are dielectrics, the bilayer structure can be scaled down to μm, giving the same beaming response also in the optical regime.

2. Systems and investigation methods

The schematic of a double bilayers structure is presented in Fig. 1(a). The first layer of each bilayer consists of 35 alumina circular rods with a lattice constant of $\alpha = 11$ mm, while the second layer of square alumina rods with lattice constant $b = 2\alpha$ (dimensions in Fig. 1 label). The distance between the circular and the square rods is equal to α and the dielectric constant of rods is equal to 9.6. The distance between the cascading bilayers is d and much larger than the lattice constant, varying between $10b$ and $30b$. The experimental setup is presented in Fig. 1(b). It consists of an HP E8364B network analyser, a horn antenna as the transmitter and a dipole antenna as the receiver. The horn antenna transmits a Gaussian beam with E polarization (the electric field parallel to the dielectric rods) and the dipole antenna scans the 2D experimen-
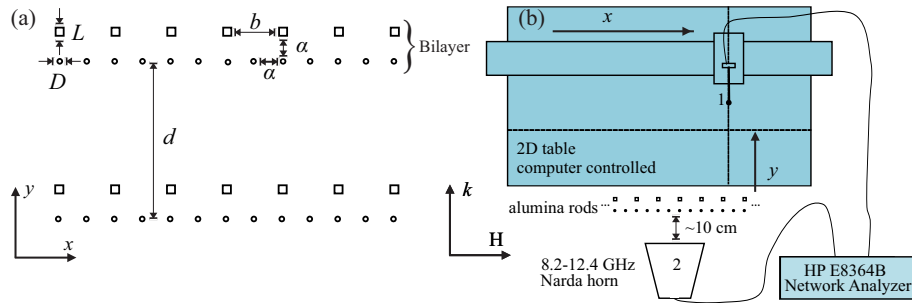
Fig. 1. (a) Schematic of a double bilayer structure. Each bilayer is composed of a surface layer of dielectric cylindrical rods, diameter $D = 1.83$ mm, and a grating layer made of rectangular rods, side length $L = 3.15$ mm.(b) Experimental configuration.

tal table, measuring the intensity of the local field close to the structure and the propagation, diffraction and interference of the outgoing waves. The scanning area of the receiver covers the front face of the dielectric rods along the lateral direction and extends to 0.76 m along the propagation direction. The numerical investigation of the structure is conducted via the commercial finite element method software COMSOL MULTIPHYSICS [16].

3. Numerical investigation of a single layer of dielectric rods

Our study begins by exploring the properties of the surface states or guided waves supported by a single layer of dielectric cylindrical rods. i.e waves bound to the interface between the dielectric rods and the air; here in after this layer is referred as surface layer. We keep the term surface (rather than guided) to characterize these modes as more general and linking to the existing studies of beaming in PCs and plasmonic systems. The band structure of the surface
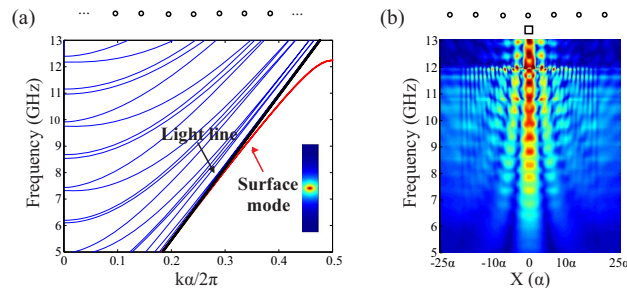

Fig. 2. (a) Band structure of an infinite layer of cylindrical rods (structure drawing on top of the plot). The black line shows the light line and the red curve corresponds to the dispersion of the surface mode. Inset shows the field distribution of the surface mode. (b) Profile of the local field for the finite surface layer. The structure consists of the finite surface layer and a single square scatterer placed before the surface layer, at distance equal to α (structure drawing on top of the plot). The local field is calculated at a short distance, equal to $\alpha/2$, behind the surface layer within the frequency range of 5-13 GHz.

mode in an infinite surface layer can be identified by employing a large enough supercell in the plane wave expansion method [17] and it is presented in Fig. 2(a). The dispersion curve of the evanescent surface states is found to lie below the light cone in the range of 7.5-12.2 GHz and the field distribution of the mode is presented in the inset of Fig. 2(a). Given that these states are characterized by a zero k perpendicular component, they cannot be excited by a normally

incident plane wave. Initially, for the investigation of the surface waves in the finite surface layer of the bilayer under consideration, a single square rod is place between the source antenna and the surface layer. Diffraction form the single rod allows for the generation of waves that have all k parallel components. These diffracted waves can couple with the surface mode and propagate along the lateral direction. Numerical simulations for this configuration are presented in Fig. 2(b); here the profile of the field at the front face of the finite surface layer within the frequency range of 5-13 GHz is demonstrated. As shown surface waves are excited for frequencies greater than 7 GHz, their intensity is enhanced as frequency increases and reaches a maximum at 11.8 GHz. For greater frequency values the surface modes are suppressed. The surface profile of the finite layer following the single square rod stands in accordance with the band structure of the infinite layer. Some discrepancy is attributed to the finite number of rods of the surface layer.

4. Experiments and simulations of beaming in a bilayer structure and in multiple cascading bilayers

The surface wave leads to wider field distribution and reduced transmission along the propagation direction and in order to achieve enhanced beaming, the surface energy needs to be converted into outgoing radiation. This is achieved by adding the grating-like second layer. The grating layer apart from enabling the excitation of the surface waves allows for the coupling of their energy to radiation modes, which translates into the improved beaming of the outgoing field. Each rod diffracts the surface energy and the beaming is a result of constructive inter-
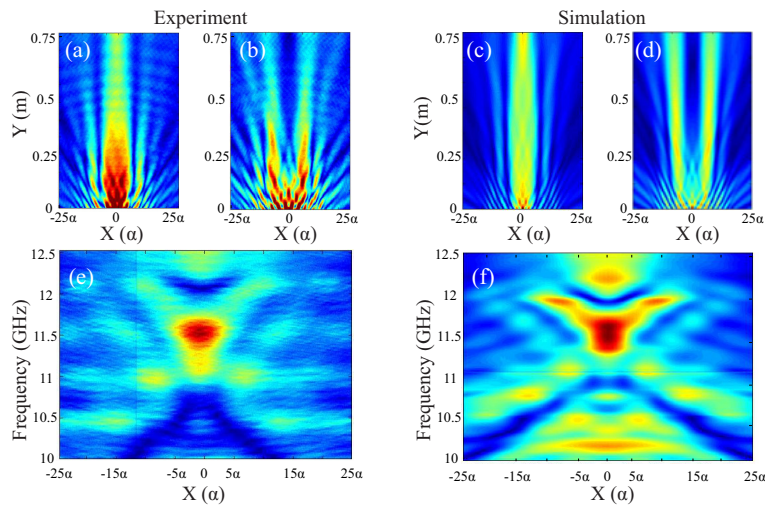

Fig. 3. Experimental 2D strength plot of the outgoing field at (a) 11.55 GHz and (b) 12.04 GHz, (c) and (d) corresponding numerical simulations for the one bilayer case. (e) Experimental x cross section strength profile of the field measured at the y end of the experimental table (0.7 m from the sample) in the range 10-12.5 GHz and (f) corresponding simulation.

ference in the forward direction. The physical origin of the beaming is the same as thoroughly discussed in [11].The experimental and numerical study of the bilayer structure is presented in Fig. 3. The rods are placed at a fixed distance away from the horn antenna and the receiver scans the bilayer posterior area both in x and y directions and in the frequency range of 10-12.5 GHz. Figure 3(e) demonstrates the x cross section strength profile of the field measured at the y end of the experimental table (0.7 m away from the sample) with respect to the frequency. The corresponding simulated profile is presented in Fig. 3(f); experimental and theoretical data stand in

good agreement. The results indicate that bilayer is characterized by a dispersive ability to provide good convergence and beaming. As shown, in the frequency range of 11.2-11.8 GHz the field distribution is narrow and the intensity is high, that is beaming is optimum. For lower and higher frequencies the field distribution becomes wider and at certain values the beam may also spilt. Figures 3(a)–3(d) demonstrate the experimental and simulated 2D profile of the outgoing field and at the optimum frequency of 11.55 GHz, where the good converge and beaming is observed, and at the frequency of 12.04 GHz, where beam splitting occurs. The 2D plot begins from the front face of the grating layer and extends to 0.7 m along the propagation direction. Looking at the proximity of the grating layer, is it observed that the normally incident field is diffracted form the grating rods and constructive inference of the diffracted waves leads to the formation of the beam at the aforementioned frequency range.
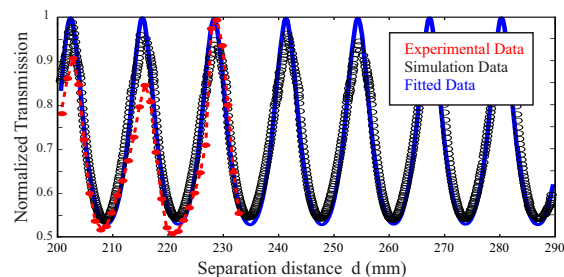

Fig. 4. Normalized transmission of the two bilayer structure with respect to the separation distance d, experimental (red curve), simulated (black curve) and fitted data (blue curve).

The optimum beaming frequency 11.55 GHz is selected as the working frequency for the design of a double bilayer system. Two identical bilayers are placed at a variable, and yet to be determined, separation distance d and the source is normally incident to the first bilayer. The area between the two bilayers acts as a Fabry-Perot cavity which ensures high transmission, while the second bilayer cancels the divergence of the beam and provides enhanced collimation for the outgoing field at the designed frequency. Figure 4 presents the transmission of the two bilayer case as a function of the separation distance d. The transmission is calculated as the line integral of the normalized field at the y end of the experimental table. The red curve corresponds to the experimental data, while the black curve represents the simulated transmission; the results stand in good agreement. Assuming that the beam diverges slowly during the propagation, the transmission properties of the two bilayer system can be interpreted analytically based on the one mode assumption [15, 18]. The fitted data are presented in Fig. 4 (blue curve) and as the results indicate, the transmission is a periodic function of the separation distance d; the period is equal to $\lambda/2$ (13 mm) of the working wavelength. The transmission maxima are found at d = 202 mm, 215 mm, ..., 202 mm + $n\lambda/2$, n being an integer. Given the restricted divergence of the field (Fig. 3(a)) and the good agreement between the experiment and the theory it is safe to say that the transmission function can be extrapolated at larger separation distance d.

For the experimental investigation of the double bilayer structure we choose the separation distance d to be equal to 566 mm. The receiver dipole antenna scans the area between the two bilayers, omits the area where the second bilayer stands and the measurement is completed by scanning the area following the second bilayer. Like in the single bilayer case, Fig. 5(a) presents the x cross section profile of the field strength measured at the maximum propagation distance of the experimental table (0.7 m away from the sample) as a function of the frequency (10-12.5 GHz); the results are numerically verified by the corresponding simulation shown in Fig. 5(b). As expected the optimum convergence occurs at 11.55 GHz. Figures 5(c) and 5(d) present the 2D profile of the field at the working frequency. Close to the grating layers one

observes the diffraction and the interference of the waves, between the two bilayers the Fabry-Perot phenomena and at the exit of the second bilayer the collimation of the beam. Enhanced
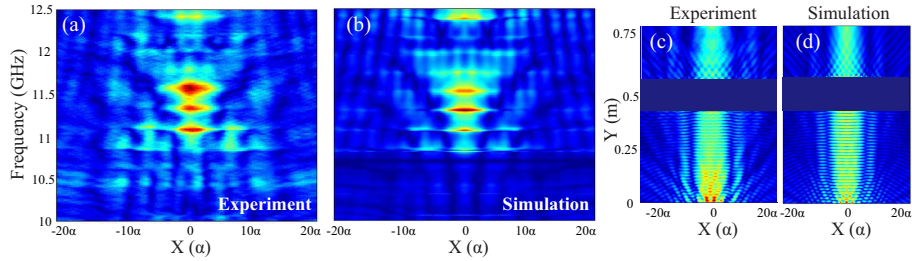

Fig. 5. (a) Experimental *x* cross section strength profile of the field measured at the end of the experimental table within the range of 10-12.5 GHz and (b) correspond numerical simulation. (c) Experimental 2D strength plot of the outgoing field at the optimum frequency 11.55 GHz and (b) corresponding numerical simulations for the two bilayer case.

collimation and transmission can be achieved by using multiple cascading bilayers. Figures 6(a) and 6(b) presents the simulated 2D plot of the field strength for a structure of two bilayers and a structure of four bilayers at 11.55 GHz and figure 6(c) plots the normalized field distribution of the two structures at a propagation distance equal to 2.6 m (100λ). It is obvious that the four bilayer is capable of cancelling the divergence of the beam and provides better transmission.
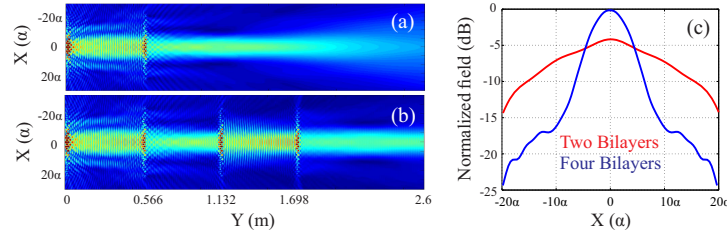

Fig. 6. Simulation of the 2D field strength for the case of (a) two bilayer and (b) four bilayer structure. (c) Normalized *x* cross section field distribution for the two and four bilayer case at a propagation distance of 100λ.

5. Conclusions

In this work, we have demonstrated experimentally and theoretically that under certain circumstances the transmission of a Gaussian beam through a bilayer dielectric structure can result in enhanced transmission and beaming. Moreover by arranging multiple cascading bilayers one can ensure the repeatedly refocusing of the beam and the high transmission at large distances. Due to its simple design, the bilayer has a discrete advantage in all practical applications related with non-diffractive propagation, guiding and steering of the electromagnetic radiation, including long distance wireless energy propagation, coupling of optical elements etc.